Heterometallic Homo- and Heteroleptic Porphyrinate Dimers with a Rhodium−Thallium Bond

Dimitra Daphnomili,[†] W. Robert Scheidt,[‡] Jaroslav Zajicek,[‡] and Athanassios G. Coutsolelos*,[†]

Department of Chemistry, Laboratory of Bioinorganic Coordination Chemistry, School of Sciences, University of Crete, P.O. Box 1470, 714 09 Heraklion, Crete, Greece, and Department of Chemistry and Biochemistry, University of Notre Dame, Notre Dame, Indiana 46556

Received November 5, 1997

The synthesis and spectroscopic characterization of four heterometallic porphyrinate dimers containing rhodium−thallium metal−metal bonds are reported. The investigated compounds are represented by the formula (Porph)Rh−Tl(Porph′), where Porph and Porph′ are OEP and/or TPP. UV/visible spectroscopy of the title complexes confirms the presence of a strong $\pi-\pi$ interaction between the macrocycles in each derivative. With ^{1}H and ^{13}C NMR data, we were able to distinguish two major NMR regions: the *endo*, between the metal−metal bonded macrocycles, and the *exo*, outside the macrocycles, which are characteristic features of porphyrinic dimers. ^{205}Tl NMR for the title complexes was performed, and the chemical shifts of the thallium nucleus are presented. For the four complexes, the magnitudes of spin−spin coupling constants between thallium and rhodium nuclei have been measured for the first time. Finally, reactions with selected substrates were studied in order to investigate the reactivity as well as the polarity of the metal−metal bond.

Introduction

Dimeric metalloporphyrins are assembled by using a diversity of links, such as formation of a bridge between two metals by a bridging ligand,[1] a covalent bond at the porphyrin ligand periphery resulting in a cofacial configuration,[2] and a direct metal−metal bond.[3]

The last class has received considerable attention. A large number of porphyrin compounds that contain metal−metal multiple bonds have been investigated in terms of structure and bonding.[3b,d] However, this is not the case for dimeric porphyrins that possess metal−metal single bonds. In fact, the homometallic dimers of Rh[4] and Ir[5] are the only ones appearing in the literature. The only dimers known, to date, with a bond between a transition and a nontransition metal are those with a Rh−In bond.[6] The metal−metal bond in those dimers exhibits σ-character and a directed polarization from rhodium to indium (formally Rh(I): → In(III)).[6b] Continuing the effort to investigate the nature and properties of this kind of metal−metal bond, we report herein the synthesis and characterization of a new series of heterometallic homo- and heteroleptic dimers that contain Rh−Tl bonds. The two porphyrin ligands used in this work are the octaethylporphyrin dianion (OEP^{2-}) and the tetraphenylporphyrin dianion (TPP^{2-}). Each of these ligands imparts different electronic as well as steric effects on the metal center (due to their peripheral substituents), and it is possible to modify indirectly the properties of the metal−metal bond formed.

Experimental Section

General Information. All chemicals were reagent grade and were used without further purification, except as noted. Basic, type I alumina was activated at 150 °C for a minimum of 24 h. THF and toluene were distilled over sodium/benzophenone under an inert atmosphere. Spectra for extinction coefficient measurements were recorded in toluene (Merck spectral grade). Ethanol and the basic aqueous solution (0.5 M) of $NaBH_4$ were degassed via three freeze−pump−thaw cycles. Manipulation of oxygen-sensitive compounds (reduced Rh(I) porphyrinic species with OEP or TPP) was carried out on a vacuum line under an argon atmosphere using Schlenk tube techniques. All manipulations of light-sensitive derivatives were carried out in the darkroom (metal−metal bonded dimers).

* To whom correspondence should be addressed. Phone: ++30.81.393636. Telefax: ++30.81.210951 or 393671 PC modem. Internet: coutsole@ikaros.edu.uch.gr.

[†] University of Crete.

[‡] University of Notre Dame.

(1) (a) Summerville, D. A.; Cohen, I. A. *J. Am. Chem. Soc.* **1976**, *98*, 1747. (b) Chin, D.-H.; La Mar, G. N.; Balch, A. L. *J. Am. Chem. Soc.* **1980**, *102*, 4344. (c) Mansuy, D.; Lecomte, J.-P.; Chottard, J.-C.; Bartoli, J.-F. *Inorg. Chem.* **1981**, *20*, 3904. (d) Shin, K.; Yu, B.-S.; Goff, H. M. *Inorg. Chem.* **1990**, *29*, 889.

(2) (a) Collman, J. P.; Kim, K.; Garner, J. M. *J. Chem. Soc., Chem. Commun.* **1986**, 1711. (b) Collman, J. P.; Garner, J. M. *J. Am. Chem. Soc.* **1990**, *112*, 116.

(3) (a) Collman, J. P.; Barnes, C. E.; Collins, T. J.; Brothers, P. J.; Gallucci, J.; Ibers, J. A. *J. Am. Chem. Soc.* **1981**, *103*, 7030. (b) Collman, J. P.; Arnold, H. J. *Acc. Chem. Res.* **1993**, *26*, 586 and references therein. (c) Collman, J. P.; Arnold, H. J.; Fitzgerald, J. P.; Weissman, K. *J. Am. Chem. Soc.* **1993**, *115*, 9309. (d) Collman, J. P.; Woo, L. M. *Proc. Natl. Acad. Sci. U.S.A.* **1984**, *81*, 2592.

(4) (a) Ogoshi, H.; Setsune, J.; Yoshida, Z. *J. Am. Chem. Soc.* **1977**, *99*, 3869. (b) Setsune, J.-I.; Yoshida, Z.-I.; Ogoshi, H. *J. Chem. Soc., Perkin Trans. 1* **1982**, 983. (c) Collman, J. P.; Ha, Y.; Guilard, R.; Lopez, M.-A. *Inorg. Chem.* **1993**, *32*, 1788. (d) Ni, Y.; Fitzgerald; J. P.; Carroll, P. J.; Wayland, B. B. *Inorg. Chem.* **1994**, *33*, 2029. (e) Lee, S.; Mediati, M.; Wayland, B. B. *J. Chem. Soc., Chem. Commun.* **1994**, 2299.

(5) Del Rossi, K.; Wayland, B. B. *J. Chem. Soc., Chem. Commun.* **1986**, 1653.

(6) (a) Jones, N. C.; Carroll, P. J.; Wayland, B. B. *Organometallics* **1986**, *5*, 33. (b) Coutsolelos, A. G.; Lux, D.; Mikros, E. *Polyhedron* **1996**, *15*, 705. (c) Lux, D.; Daphnomili, D.; Coutsolelos, A. G. *Polyhedron* **1994**, *13*, 2367.

S0020-1669(97)01393-1 CCC: $15.00
Published on Web 07/01/1998

Synthesis of [(Porph)M^{III}Cl]. The complexes [(Porph)Rh^{III}Cl] and [(Porph)Tl^{III}Cl] were prepared according to literature methods.[7,8]

Synthesis of [(Porph)Rh^{I}]$^-$. The reduction of [(Porph)Rh^{III}Cl] (where Porph = OEP, TPP) was achieved by a slight modification of a previously published procedure.[9] [(Porph)Rh^{III}Cl] (0.04 mmol) was dissolved under an argon atmosphere in 25 mL of oxygen-free ethanol. The solution was heated to 50 °C, and a basic aqueous solution of $NaBH_4$ (1.04 mmol) was slowly added. The solution was stirred vigorously for 1 h. The formation of the rhodium(I) porphyrin was monitored by UV/visible spectroscopy.[4b] After complete formation of the desired reduced complex, the solvent was removed under vacuum, and the crude solid was used directly for the next step, which is the nucleophilic attack of [(Porph)Rh]$^-$ on a [(Porph)M^{III}Cl] derivative and the formation of the corresponding dimer.

Synthesis of (OEP)Rh−Tl(OEP). [(OEP)Tl^{III}Cl] (0.04 mmol) was dissolved under an argon atmosphere in 30 mL of freshly distilled THF. The solution was transferred to the solid residue of [(OEP)Rh^{I}]$^-$, and the mixture was stirred for 0.5 h at room temperature in the dark. The solution was evaporated, and the crude product was passed through an Al_2O_3 column (4 × 2 cm, type I Basic), also in the dark. The porphyrin dimer was eluted with toluene as the eluent (yield 20%, based on [(OEP)Rh^{III}Cl]).

Synthesis of (TPP)Rh−Tl(OEP). [(OEP)Tl^{III}Cl] (0.04 mmol) was dissolved under an argon atmosphere in 30 mL of freshly distilled THF. The solution was added to the freshly prepared, solid [(TPP)Rh^{I}]$^-$, and the mixture was stirred for 0.5 h at room temperature in a dark room. The solvent was evaporated, and the crude solid was chromatographed on an Al_2O_3 column (4 × 2 cm, type I Basic) in the dark. The porphyrinic dimer was eluted first with toluene as the eluent (yield 43%, based on [(TPP)Rh^{III}Cl]).

Synthesis of (TPP)Rh−Tl(TPP). [(TPP)Tl^{III}Cl] (0.04 mmol) was dissolved under an argon atmosphere in 30 mL of freshly distilled THF. The solution was transferred to the solid residue of [(TPP)Rh^{I}]$^-$, and the mixture was stirred for 0.5 h at room temperature and in the absence of light. The solution was evaporated, and the crude product was chromatographed on an Al_2O_3 column (6 × 2 cm, type I Basic) in the dark and with toluene as the eluent. The first fraction contained free base $(TPP)H_2$ and a tetraphenylthallium porphyrin derivative which was formed during the reaction, as will be discussed later. The desired dimer was obtained in the second fraction of the eluate (yield 23%, based on [(TPP)Rh^{III}Cl]).

Synthesis of (OEP)Rh−Tl(TPP). The reaction for the formation of this dimer was similar to those described above. However, the purification of the complex required two chromatographic separations of the reaction mixture. In the first, a mixture of $(TPP)H_2$ with the desired dimer was eluted with a mixture of solvents (toluene/hexane, 1:1 v/v) as eluent. After evaporation of the solvent, this fraction was passed through an Al_2O_3 column (7 × 2 cm, type I Basic). Free base was eluted first with a mixture of toluene/hexane (1:1−3:2 v/v). Analytically pure dimer (OEP)Rh−Tl(TPP) was collected in the second fraction with toluene as the eluent (yield 15%, based on [(OEP)Rh^{III}Cl]).

NMR Instrumentation. Varian UNITY*plus* 300-MHz and Varian VXR-500S 500-MHz spectrometers were used to measure ^{1}H, ^{13}C, and ^{205}Tl NMR spectra. The experiments were carried out on 1×10^{-5} M $CDCl_3$ solutions. The ^{13}C and ^{205}Tl spectra were acquired with WALTZ ^{1}H decoupling. Chemical shifts are reported in δ (ppm) using TMS as an internal standard for the ^{1}H and ^{13}C spectra. The resonance signal of $Tl^{III}(NO_3)_3$ obtained in D_2O solution was used as an external standard for the ^{205}Tl spectra. The ^{13}C spin−lattice relaxation times, T_1, for (TPP)Rh−Tl(OEP) were measured with proton decoupling using the inversion recovery technique[10] at −30 and +30 °C. At least 14 different τ values were used, and the waiting period between successive acquisitions was at least 2−3 times the longest T_1 time measured. The values of the relaxation times were obtained from three parameter fits to the row data.[11]

UV/Visible Instrumentation. Absorption spectra were collected on a Perkin−Elmer Lambda 6 spectrophotometer or on a diode-array spectrometer adapted for our experiments with components from the ORIEL Co. Spectra for extinction coefficient measurements were recorded in toluene (5×10^{-5} M solutions).

Results and Discussion

Synthesis. Several methods have been developed for the synthesis of singly bonded metal−metal dimers, such as photolysis[12] and thermolysis,[4a] which require (porphinato)-rhodium hydride in an intermediate step. The synthesis of (Porph)Rh−Tl(Porph′) [where (Porph) = OEP or TPP and (Porph) = or ≠ (Porph′)] was performed in an alternate way, via a two-step reaction, by omitting the formation of the hydride. In this synthetic procedure, the direct nucleophilic attack of [(Porph)Rh^{I}]$^-$ on [(Porph)Tl^{III}Cl] gives rise to the formation of a rhodium−thallium single bond. The synthetic procedure followed was similar to that used for the (Porph)-Rh−In(Porph′) complexes. The following equation represents the general reaction scheme for the synthesis of this new family of complexes:

$$[(\text{Porph})\text{Rh}^{\text{I}}]^-\text{Na}^+ + (\text{Porph}')\text{Tl}^{\text{III}}\text{Cl} \xrightarrow[\text{THF}]{\text{in the dark}} (\text{Porph})\text{Rh}-\text{Tl}(\text{Porph}')$$

(Porph and Porph′ = OEP, TPP)

A comparison with the similar rhodium−indium derivatives shows a few peculiarities concerning the synthetic process of these rhodium−thallium dimers. In the reaction mixture for the synthesis of (Porph)Rh−Tl(TPP) derivatives, an intermediate species is detected (Soret band at 460 nm in THF (under Ar) and 480 nm in toluene). The electronic spectrum is similar to that of [(TPP)Tl^{I}]$^-$,[13] which leads to the suggestion that reduction of [(TPP)Tl^{III}Cl] takes place during the reaction. This reduction leads to the thallium(I) derivative, [(Porph)Tl$^{I}_2$], followed by its demetalation.[13] This gives rise to the free base, a well-known feature of the chemistry of Tl(I) porphyrinates. Note that this reduction is observed only when thallium(III) is coordinated to tetraphenylporphyrin. A reasonable explanation is the different reduction potentials ($E_{1/2}$) of the two thallium complexes.[14]

Reduction of the rhodium(III) derivative occurs under strictly anaerobic conditions and can be monitored by UV/visible spectroscopy. It is to be noted that, during the preparation of the [(Porph)Rh^{III}Cl] derivatives, the [(Porph)Rh^{III}C$_8$H$_{13}$] complex is also formed. When traces of this organorhodium complex are present with [(Porph)Rh^{III}Cl], it is impossible to extract, in pure analytical form, the desired dimer containing the Rh−Tl bond. The synthesis of the metal−metal dimers as well as their chromatographic purification requires absolute darkness. Purification follows different procedures, depending on whether free base $(TPP)H_2$ and the thallium(I) tetraphenylporphyrin derivative are in the reaction mixture. Note also that unreacted $NaBH_4$ could reduce [(TPP)Tl^{III}Cl] as a side reaction (in the second step) of the synthetic procedure.

(7) Abraham, R. J.; Barnett, G. H.; Smith, K. M. *J. Chem. Soc., Perkin Trans. 1*, **1973**, 2142.
(8) Sadasivan, N.; Fleischer, E. F. *J. Inorg. Nucl. Chem.* **1968**, *30*, 591.
(9) Ogoshi, H.; Setsune, J.; Omura, T.; Yoshida, Z. *J. Am. Chem. Soc.* **1975**, *97*, 6461.
(10) Martin, M. L.; Martin, G. J.; Delpuech, J. J. *Practical NMR Spectroscopy*; Heyden: London, 1980; Chapter 7.
(11) Weiss, G. H.; Ferretti, J. A. *Prog. Nucl. Magn. Reson. Spectrosc*. **1988**, *4*, 317.
(12) Wayland, B. B.; Newman, A. R. *Inorg. Chem.* **1981**, *20*, 3092.
(13) Smith, K. M.; Lai, J. J. *Tetrahedron Lett.* **1980**, *21*, 433.
(14) Kadish, K. M.; Tabard, A.; Zrineh, A.; Ferhat, M.; Guilard, R. *Inorg. Chem.* **1987**, *26*, 2459.

Table 1. ^{1}H NMR Data for Complexes (Porph)Rh−Tl(Porph) and (Porph)Rh−Tl(Porph)′ and Their Monomeric Precursors [(Porph)M^{III}Cl] in $CDCl_3$

	macrocycle								
	tetraphenylporphyrin[a]						octaethylporphyrin[a]		
compound	*o*-H (*exo*)	*o*′-H (*endo*)	*m*-H (*exo*)	*m*′-H (*endo*)	*p*-H	H−pyr	−CH_2−	−CH_3−	H-*meso*
(OEP)Rh-Tl(OEP)									
thallium entity							dm/16	t/24	s(b)/4
							4.07/3.84	1.66	8.99
rhodium entity							dm/16	t/24	s/4
							4.16/3.86	1.77	8.72
(OEP)Rh-Tl(TPP)									
thallium entity	d/4	d/4	t/4	t/4	t/4	s/8			
	7.11	9.07	7.42	8.19	7.79	8.30			
rhodium entity							m/16	t/24	s/4
							4.00/3.8	1.55	8.96
(TPP)Rh-Tl(OEP)									
thallium entity							dm/16	t/24	s(b)/4
							4.07/3.80	1.50	9.13
rhodium entity	dt/4	dt/4	td/4	td/4	tt/4	s/8			
	7.28	8.95	7.47	8.19	7.79	8.13			
(TPP)Rh-Tl(TPP)									
thallium entity	d/4	d/4	t/4	t/4	t/4	s/8			
	7.17	8.82	7.40	7.93	7.84	8.33			
rhodium entity	d/4	d/4	t/4	t/4	t/4	s(br)/8			
	7.33	8.68	7.48	7.93	7.73	8.28			

precursor	*o*′-H[b]	*o*″-H[b]	*m*-H	*p*-H	H−pyr	−CH_2−	−CH_3	H-*meso*
[(TPP)Tl^{III}Cl]	d/4	d/4	m/8	m/4	d/8			
	8.37	8.14	7.81	7.76	9.03			
					(64.7)[c]			
[(OEP)Tl^{III}Cl]						dm/16	t/12	d/4
						4.18/4.16	1.98	10.33
						(43.6)[c]		
[(TPP)Rh^{III}Cl]		m/8		m/12	d/8			
		8.25		7.77	8.94			
[(OEP)Rh^{III}Cl][d]						m/16	t/12	s/4
						4.13	1.98	10.32

[a] Top line of each entry first gives multiplicity (s = singlet, s(b) = singlet broad, d = doublet, m = multiplet, dt = doublets of triplets, td = triplets of doublets, tt = triplet of triplets, and dm = doublet of multiplets), followed by number of protons. The second line gives chemical shift values on the δ scale. [b] Two signals because thallium is out of the porphyrin mean plane. [c] ^{205}Tl−H coupling in hertz. [d] Spectrum in C_6D_6.

In the solid state, the complexes formed are quite stable in air and/or daylight, while in solution they are extremely sensitive to light and decompose to the corresponding five-coordinate precursors. They are very soluble in many solvents, such as CH_2Cl_2, $PhCH_3$, and C_6H_6, and quite soluble in THF, DMF, and diethyl ether.

Nuclear Magnetic Resonance Spectroscopy. ^{1}H NMR. All complexes exhibit ^{1}H NMR features characteristic for diamagnetic compounds. The proton resonances for the complexes and their corresponding monomeric precursors were assigned to individual hydrogen atoms on the basis of the interpretation of the DQF−COSY and NOESY spectra (Table 1). These metal−metal bonded dimers with cofacial porphinato rings have two well-defined regions that must be considered in the proton assignments. The region between the two macrocycles is called *endo*, while the region above one and under the other macrocycle is *exo*, see Figure 1.

It was found that the phenyl protons of the tetraphenylporphyrin (TPP) entities exhibit five separate resonance signals. Due to the ring current formed between two macrocycles, the ortho (*o*′) and meta (*m*′) protons in the *endo* region are deshielded and resonate at lower field than the corresponding protons of the monomeric precursors. The deshielding of the *o*′ protons is greater than that of the *m*′ protons. On the other hand, the ortho (*o*) and meta (*m*) protons in the *exo* region experience shielding and resonate at higher field than the corresponding protons of the monomeric precursors. The effect of the shielding is more pronounced for the ortho protons. The methylene protons of the octaethylporphyrin (OEP) entities in the dimers were found to be anisochronous, as they exhibited two separate multiplets (Table 1). The pyrrolic protons of the TPP macrocycle and the meso protons of the OEP ring resonated at higher field than in the corresponding monomers. Each group of protons gave rise to a single line, but the difference in the chemical shifts is larger for the pyrrolic protons.

Such shielding effects of the pyrrolic and meso protons have been also observed in the (Porph)Rh−In(Porph) series.[6b,c] Shielding and deshielding is also observed in (Porph)Tl−CH_3[14] and (Porph)Tl−M(L)$_n$[15bc] and is consistent with σ-character of the metal−metal bond as well as with the electron-donating or -withdrawing ability of the [(Porph)Rh^I]$^-$ unit. If we compare the chemical shifts of the thallium complexes with those of the (Porph)Rh−In(Porph)[6b,c] series, we observe that the differences are found mainly for the protons near the centers of magnetic anisotropy. For example, the *meso* protons of the (OEP)Tl unit are more shielded ($\Delta\delta$ 1.36) than the corresponding protons in the indium series ($\Delta\delta$ 1.10). The small difference suggests that the presence of the second macrocycle is the main center of

(15) (a) Guilard, R.; Mitaine, P.; Moise, C.; Lecomte, C.; Boukhris, A.; Swistak, C.; Tabard, A.; Lacombe, D.; Cornillon, J.-L.; Kadish, K. M. *Inorg. Chem.* **1987**, *26*, 2467. (b) Guilard, R.; Zrineh, A.; Ferhat, M.; Tabard, A.; Mitaine, P.; Swistak, C.; Richard, P.; Lecomte, C.; Kadish, K. M. *Inorg. Chem.* **1988**, *27*, 697. (c) Guilard, R.; Tabard, A.; Zrineh, A.; Ferhat, M. *J. Organomet. Chem.* **1990**, *389*, 315.

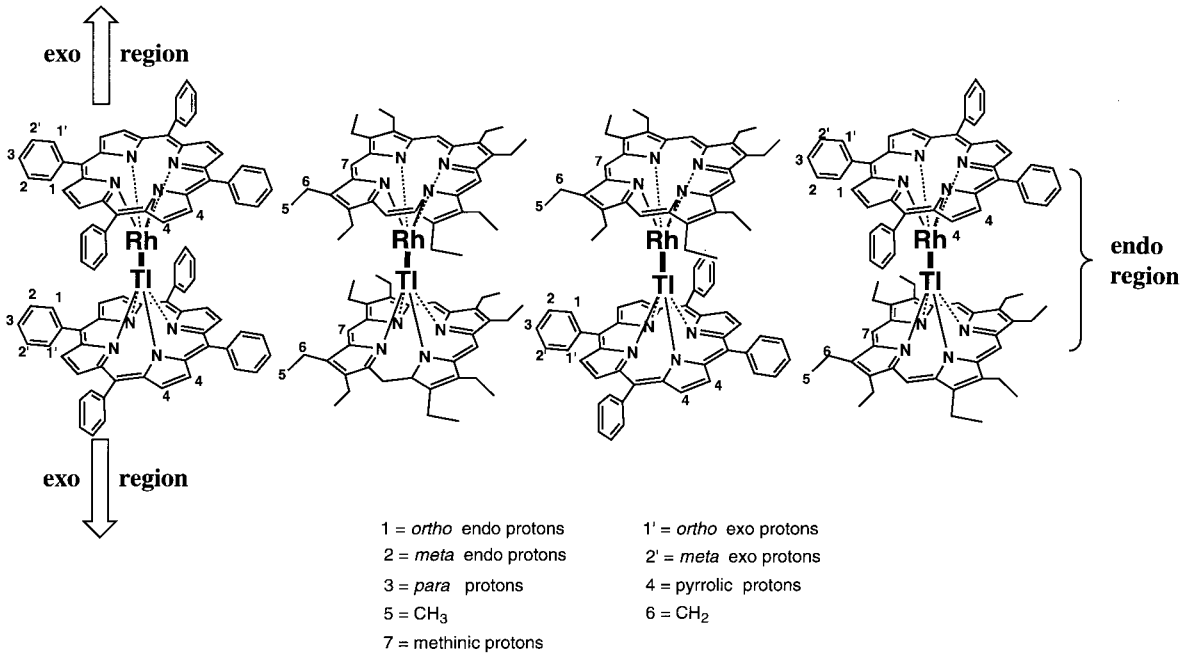

Figure 1. Four combinations of porphyrin rings containing a Rh−Tl bond, their NMR regions, and the different kind of protons.

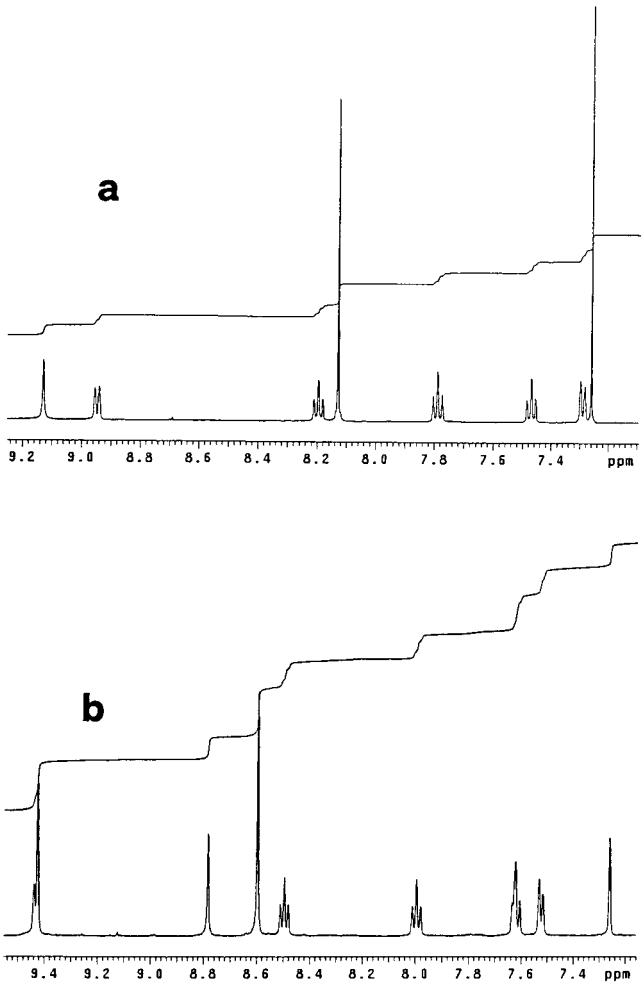

Figure 2. ^{1}H NMR spectra of (OEP)Rh−Tl(TPP) in $CDCl_3$ (a) and pyridine-d_5 (b); only the aromatic region is shown.

magnetic anisotropy. These differences can reflect a change of the distance between the two macrocycles, which is expected due to the larger displacement of thallium from the mean porphyrin plane compared to that of indium. Such differences are observed in monomeric complexes of indium[15a,16] and thallium.[17]

As reported in the literature,[7,18] Tl−H couplings were observed between Tl(III) and the *meso* or *pyrrolic* protons of the porphyrin macrocycle. The magnitude of the coupling was dependent on the porphyrin electron density and on the nature of the axial ligand. The interaction between the *meso* or *pyrrolic* protons and the Tl is stronger when the group bound to the Tl possesses some electron-withdrawing ability. Thus, in the series of (Porph)Tl−R derivatives, where R is an electron-donating group, no Tl−H couplings were observed.[14] In the [(Porph)-Rh−Tl(Porph)] series, the (OEP)Rh−Tl(OEP) is the only complex in which the *meso* protons of the Tl entity exhibit a 0.5-Hz coupling with the thallium. The absence of or a very small coupling may be correlated with the polarization of the Rh−Tl bond. In the (OEP)Rh−Tl(OEP) dimer, the $[(Porph)Rh^{I}]^-$ acts as an electron donor to the Tl atom, influencing the scalar spin−spin interaction of the Tl with the *meso* and *pyrrolic* protons.

^{13}C NMR. ^{13}C NMR spectra were measured for all Rh−Tl derivatives and the monomeric precursors. Assignments of signals derived from all proton-bearing carbons of the Rh−Tl dimers were made by analyzing the HETCOR spectra and are given in Table 2. The signals derived from the quaternary carbons were assigned by comparison with $^{13}C\{^1H\}$ spectra of the corresponding monomeric precursors (Table 2). For all dimers, except, of course, the (OEP)Rh−Tl(OEP) derivative, two signals were observed for both the ortho and the meta phenyl carbons. These were assigned to *o′*- and *m′-endo* and *o*- and *m-exo* carbons on the basis of their correlation with corresponding proton resonances.

(16) Lecomte, C.; Protas, J.; Cocolios, P.; Guilard, R. *Acta Crystallogr. Sect. B* **1980**, *36*, 2769.
(17) (a) Henrick, K.; Matthews, R. W.; Tasker, P. A. *Inorg. Chem.* **1977**, *16*, 3293. (b) Brady, F.; Henrick, K.; Matthews, R. W. *J. Organomet. Chem.* **1981**, *210*, 281. (c) Senge, M. O.; Senge, K. R.; Regli, K. J.; Smith K. M. *J. Chem. Soc., Dalton Trans.* **1993**, 3519.
(18) Janson, T. R.; Katz, J. J. In *The Porphyrins*, Dolphin, D., Ed.; Academic Press: New York 1978; Vol. IV, Chapter 1 and references therein.

Table 2. ^{13}C NMR Chemical Shifts for Complexes (Porph)Rh−Tl(Porph) and (Porph)Rh−Tl(Porph′)[a]

carbon	(TPP)Rh−Tl(OEP)	(OEP)Rh−Tl(OEP)	(OEP)Rh−Tl(TPP)	(TPP)Rh−Tl(TPP)
C_a	145.5/150.2	139.4	142.9/148.7	146.2/148.8
C_{phenyl}	138.2		140.0	141.5/142.2
C_{o-endo}	134.0		134.7	134.6/135.2
C_{o-exo}	135.1		135.8	134.9/135.5
C_b	130.0/142.0	145.5	139.6/129.7	130.7/130.2
C_{p-}	127.0		126.9	127.1/127.3
C_{m-exo}	126.3		126.2	126.5/126.2
C_{m-endo}	126.1		125.9	126.3/126.1
C_{meso}	120.7/97.5	98.1/∼ 96	98.3/119.9	120.7/121.0
$-CH_3$	19.8	19.9/19.8	20.1	
$-CH_2-$	17.9	18.3/18.4	18.0	

[a] When a column has two values separated by "/", the first value is for the Rh entity, while the second is for the Tl entity.

Table 3. ^{13}C Spin Lattice Relaxation Times, T_1, for (TPP)Rh−Tl(OEP) in $CDCl_3$

		NT_1 (s)[a]	
carbon	δ (ppm)	−30 °C	+30 °C
		TPP	
o-endo	133.8	0.28 ± 0.02	0.42 ± 0.04
o-exo	134.9	0.28 ± 0.02	0.37 ± 0.03
pyrrolic	129.8	0.19 ± 0.01	0.28 ± 0.02
p-	126.7	0.20 ± 0.03	0.30 ± 0.02
m-exo	126.3	0.29 ± 0.02	0.38 ± 0.03
m-endo	126.1	0.25 ± 0.02	0.37 ± 0.03
		OEP	
CH_2	19.6	0.29 ± 0.01	0.51 ± 0.02
CH_3	17.6	1.25 ± 0.03	2.8 ± 0.1

[a] *N* is the number of directly attached protons to an individual carbon. Presenting the data as the NT_1 product accounts for the different number of protons of the methine, methylene, and methyl groups and allows direct comparison of relaxation.

In contrast to the monomeric Tl(III) precursors, the ^{13}C NMR spectra of the dimers did not exhibit any ^{13}C−Tl scalar coupling. This is probably due to the electron donor ability of the Rh(I), which is directly attached to the Tl(III) and, consequently, could disturb its electron density.

^{13}C spin−lattice relaxation times, T_1, for (TPP)Rh−Tl(OEP) as a representative example, were measured at a magnetic field strength of 11.7 T (125.7 MHz, ^{13}C) at −30 and 30 °C. The data provide information on the dynamic behavior of the molecule on the NMR time scale. The T_1 times (Table 3) of all carbons increased with temperature. For the (TPP)Rh entity, the T_1 value for the *pyrrolic* carbon is within the experimental error equal to the T_1 value of the *para* carbon. The T_1 values of both sets *ortho* and *meta* carbons were also the same within experimental errors, but they were higher than those of the *pyrrolic* and *para* carbons. This fact demonstrates that the phenyl ring undergoes an internal reorientation about its 2-fold symmetry axis. The relaxation of the methylene and methyl carbons of the (OEP)Tl entity is faster than that of the TPP carbons and is indicative of overall higher internal mobility of the ethyl fragment compared to that of the phenyl ring. Similar behavior has been observed in comparable dimeric metalloporphyrins.[19]

^{205}Tl NMR. Thallium possesses[20] two stable isotopes, ^{203}Tl and ^{205}Tl; both have nuclear spin $^1/_2$. As the natural abundance of the ^{205}Tl (70.5%) is higher than that of the ^{203}Tl (29.5%), we have measured the NMR spectra of the former isotope. The chemical shift of the ^{205}Tl nucleus extends over 7000 ppm. The large chemical shift range is due to a dominance of the paramagnetic term in the nuclear screening constant. Also, the range of the scalar spin−spin couplings is large. For example, one-bond ^{205}Tl−^{13}C couplings can be as large as 10 000 Hz, while a six-bond coupling of 66 Hz has been observed between ^{205}Tl and ^{1}H in certain organothallium compounds.[20] Although the ^{59}Co nucleus has a total chemical shift range of 18 000 ppm and would, thus, appear to be more sensitive to chemical shift effects than ^{205}Tl, the chemical shift in compounds in which Co and Tl are in similar environments suggests that ^{205}Tl has a larger effective chemical shift range.[20]

Table 4. ^{205}Tl NMR Chemical Shifts and ^{205}Tl−^{103}Rh Coupling Constants for Complexes (Porph)Rh−Tl(Porph) and (Porph)Rh−Tl(Porph′) and ^{205}Tl NMR Chemical Shifts for the Precursors

complex	^{205}Tl[a]	^{205}Tl−^{103}Rh[b]
(TPP)Rh−Tl(OEP)	204	5100
(OEP)Rh−Tl(OEP)	222	5249
(OEP)Rh−Tl(TPP)	190	5255
(TPP)Rh−Tl(TPP)	176	5319
[(TPP)Tl^{III}Cl]	2829	
[(OEP)Tl^{III} Cl]	2844	

[a] Value of chemical shifts, δ (ppm). [b] Coupling constant (Hz).

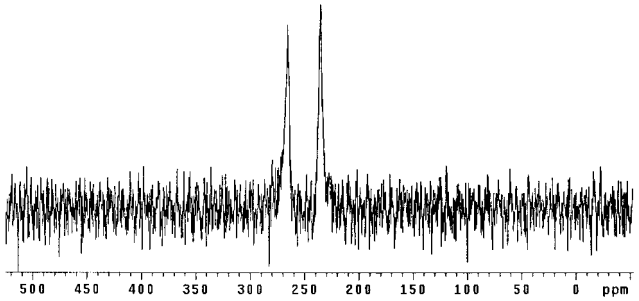

Figure 3. ^{205}Tl NMR spectrum of (OEP)Rh−Tl(OEP) in $CDCl_3$.

The ^{205}Tl NMR data for the (Porph)Rh−Tl(Porph′) dimers and their precursors are given in Table 4. The precursors exhibit greater deshielding of the ^{205}Tl nuclei and resonate at much lower field than the dimers.[21] This is probably due to the dative character of the Rh−Tl bond, although the role of the structural differences between the monomers and dimers cannot be excluded.[22] All ^{205}Tl spectra were measured with broadband proton decoupling (Figure 3). Therefore, the observed doublets (5100−5300 Hz) have been attributed to the ^{205}Tl−^{103}Rh spin−spin coupling, as natural abundance of the ^{103}Rh (spin $^1/_2$) is 100%.[23] This is the first time that Tl−Rh spin−spin couplings

(19) Coutsolelos, A. G.; Cheng, B.; Munro, O.; Zajicek, J.; Scheidt, W. R. Manuscript in preparation.
(20) Hinton, J. F.; Metz, K. R. In *NMR of Newly Accessible Nuclei*; Laszlo, P., Ed.; Academic Press: New York, 1983; Vol. 2, Chapter 14.
(21) Coutsolelos, A. G.; Daphnomili, D. *Inorg. Chem.* **1997**, *36*, 4614.
(22) Glaser, J.; Hendrikson, V. *J. Am. Chem. Soc.* **1981**, *103*, 6642.
(23) Mann, B. E. In *NMR of Newly Accessible Nuclei*; Laszlo, P., Ed.; Academic Press: New York, 1983; Vol. 2, Chapter 11.

Table 5. UV/Visible Data for Complexes (Porph)Rh−Tl(Porph) and (Porph)Rh−Tl(Porph′) and Comparison with Their Precursors[a]

compound	*B*-bands			*Q*-bands				solvent
(OEP)Rh−Tl(OEP)	341	368	408	506	563	618	642	toluene
	(4.6)	(4.9)	(4.7)	(4.0)	(3.5)	(3.3)	(sh)	
(TPP)Rh−Tl(OEP)	342		402	528	569	617		toluene
	(4.2)		(4.7)	(3.2)	(2.9)	(sh)		
(TPP)Rh−Tl(TPP)	333	366	408	524		602	648	toluene
	(4.1)	(4.1)	(4.7)	(3.4)		(3.2)	(3.2)	
(OEP)Rh−Tl(TPP)	335	382	401	514	567(sh)	614	646	toluene
(4.1)	(4.0)	(4.6)	(3.4)		(3.1)	(3.1)		
$[(OEP)Rh^{III}Cl]\cdot 2H_2O$	285	339	403	520	554			$CHCl_3$
	(4.17)	(4.26)	(5.12)	(4.12)	(4.40)			
$[(OEP)Tl^{III}Cl]$	350sh	418	498	545	582			toluene
		(5.3)	(3.3)	(4.1)	(4.0)			
$[(TPP)Rh^{III}Cl]$		421		534	567			CH_2Cl_2
		(5.0)		(4.1)	(3.7)			
$[(TPP)Tl^{III}Cl]$		434		520	566	608		toluene
		(5.5)		(3.5)	(4.1)	(4.0)		

[a] For each entry, the top line gives λ (nm) and the second line log ϵ (M^{-1} cm^{-1}).

have been observed. The magnitudes of these coupling constants are among the highest reported for thallium, ^1J(Tl−P) = 3203,[24] ^3J(Tl−H) = 3750,[25] and ^1J(Tl−C) = 5976,[26] and, to our knowledge, the largest between thallium and another metal.[27]

Electronic Absorption Data. Electronic spectroscopy proved very useful during the synthesis of these dimers. The progress of the action of the reduced species $[(Porph)Rh^{I}]^-$ on $[(Porph)Tl^{III}Cl]$ is conveniently followed with UV/visible spectroscopy. The UV/visible data for all complexes are presented in Table 5. Each dimer shows an electronic absorption spectrum that is characteristic of complexes possessing a metal−metal bond.[15] A characteristic feature of the single metal bonded complexes is the appearance of more than one absorption band in the Soret region due to the $\pi \rightarrow \pi^*$ transition of each porphyrinic entity. The formation of the dimers causes a blue shift of the highest intensity (Soret) band compared to the monomeric precursors. This band for the homoleptic OEP derivative is more blue-shifted than the heteroleptic dimers, while the Soret band of the homoleptic TPP derivative is red-shifted. The shift of the Soret band for all the complexes is related to the $\pi-\pi$ interactions of the two rings,[28] with (OEP)Rh−Tl(OEP) presenting the strongest interaction (Figure 4). The same sequence is observed for the (Porph)Rh−In(Porph′) complexes,[6b] but the Soret band displays larger shifts than the (Porph)Rh−Tl(Porph′) homoleptic derivatives. The differences in λ_{max} of the Soret bands between the two series are related to the two nontransition metals. Substitution of In by the more electronegative Tl influences mainly the splitting of the HOMOs.[28] Further, due to the different displacement of the two nontransition metals from the porphyrin mean plane, the distance of the two porphyrin rings in each series is expected to be different and larger in the Tl series. Compared to the (Porph)Rh−In(Porph′) derivatives,[6b] the bands in the blue region (300−330 nm) of the corresponding (Porph)Rh−Tl(Porph′) complexes are blue-shifted by up to 10 nm. Similar bands have been observed for the porphyrin complexes of the type (Porph)M−M′(L)$_n$ (M = In, Tl)[15] that have been attributed to the metal-to-ring transition

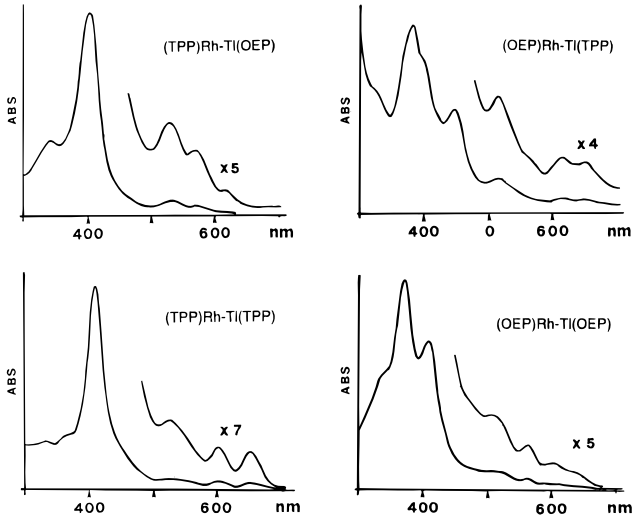

Figure 4. UV/visible data for all the complexes (Porph)Rh−Tl(Porph) and (Porph)Rh−Tl(Porph′), where Porph, Porph′ = OEP or TPP, in toluene.

$a_{2u}(n_{pz'}) \rightarrow e_g(\pi^*)$. Also characteristic for the dimers are new absorption bands appearing at longer wavelengths (λ > 600 nm) compared to the monomeric precursors. Similar low-energy bands are also found in dimers with higher bond order.[29]

Reactivity. Figure 5 describes the chemical reactivity of the (Porph)Rh−Tl(Porph′) complexes toward selected reagents. The Rh−Tl bond exhibits thermal stability in contrast to other singly bonded dimers.[30] Prolonged heating at 383 K did not cause any dissociation of the complexes. This suggests that the homolysis enthalpy is higher than that of the homometallic Rh dimers,[3d] although an exact value is not available. The thermal stability is also supported by the reactivity toward CH_3I. Reaction occurs only at high temperature (110 °C), and the exclusive products are (Porph)Rh−CH_3 and (Porph)Tl−I. The progress of the reaction was followed by UV/visible spectroscopy, monitoring the appearance of the characteristic Soret bands of the corresponding monomers. The polar character (formally Rh(I):→Tl(III)) of the Rh−Tl metal−metal bond has also been confirmed clearly by the action of I_2[4d] and CH_3I, as in the case of Rh−In derivatives[6b] (see also Figure 5).

(24) Walter, B.; Bauer, S. *J. Organomet. Chem.* **1977**, *142*, 177.
(25) Maher, J. P.; Evans, D. F. *J. Chem. Soc.* **1963**, 8590.
(26) Lee, A. G. *J. Chem. Soc. (A)* **1970**, 2153.
(27) (a) Wilson, W. L.; Rudolph, R. W.; Lohr, L. L.; Taylor, R. C.; Pyykko, P. *Inorg. Chem.* **1986**, *25*, 1535. (b) Sheldrick, G. M.; Yesinowski, J. P. *J. Chem. Soc., Dalton Trans.* **1975**, 870.
(28) (a) Shelnutt, J. A. *J. Phys. Chem.* **1984**, *88*, 4988. (b) Shelnutt, J. A.; Ortiz, V. *J. Phys. Chem.* **1985**, *89*, 4733. (c) Zgierki, M. Z. *Chem Phys. Lett.* **1986**, *124*, 53.
(29) (a) Collman, J. P.; Garner, J. M.; Woo, L. K. *J. Am. Chem. Soc.* **1984**, *106*, 3500. (b) Collman, J. P.; Prodolliet, J. W.; Leidner, C. R. *J. Am. Chem. Soc.* **1986**, *108*, 2916.
(30) Wayland, B. B.; Coffin, V. L.; Farnos, M. D. *Inorg. Chem.* **1988**, *27*, 2745.

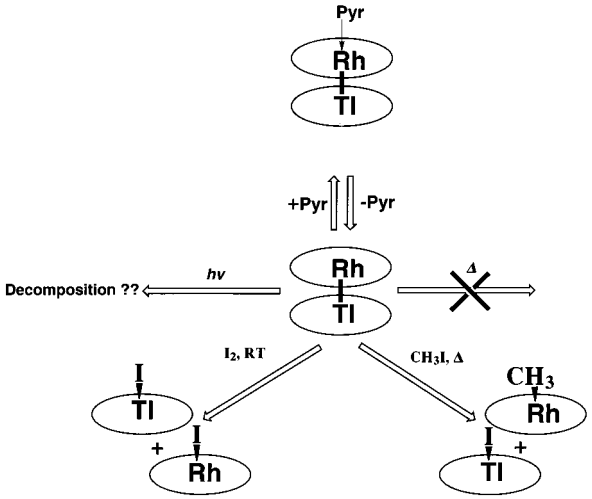

Figure 5. Overall reactivity of the title derivatives.

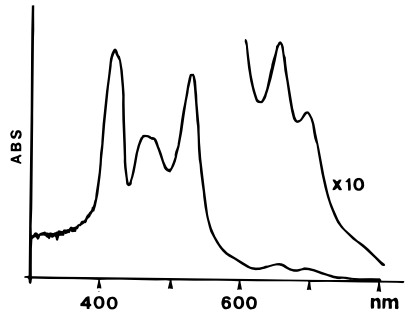

Figure 6. UV/visible spectra for (OEP)Rh−Tl(TPP) in pure pyridine.

As has been previously mentioned, all the (Porph)Rh−Tl(Porph′) complexes are soluble in solvents of various polarity. Their UV/visible spectra show no significant differences except for small, expected shifts in λ_{max} due to solvent. However, a neat pyridine solution results in dramatic changes in the UV/visible spectrum (compare Figure 6 with Figure 5, upper left). Removal of the pyridine under vacuum and in the dark and dissolution of the solid in CH_2Cl_2 results in the reappearance of the initial electronic spectrum. This behavior seems consistent with weak coordination of pyridine to one or both metals. However, titration of a CH_2Cl_2 solution of the complex with pyridine (millimoles mole of dimer/millimoles mole of pyridine 9:1−1:2000) does not show any significant change in UV/visible spectra. The spectroscopic differences are observed only in pure pyridine. The metal site of the possible pyridine binding is not obvious; neither the d^8 Rh nor the very large Tl ion is expected to have a high affinity for an additional ligand in these metal−metal bonded systems. These interesting features observed by UV/visible spectroscopy and the questions raised thus prompted us to measure ^{1}H NMR spectra of these dimers in pyridine-d_5.

The proton spectrum of, for example, (TPP)Rh−Tl(OEP) (Figure 2b) shows that the species in pyridine solution is still diamagnetic, since all resonance signals occur in the range of 0−10 ppm. Also, the dimeric nature of the complex is retained, since we observe *endo* and *exo* resonances for the phenyl protons. This is different from the case of $[(Porph)Rh]_2$ complexes,[3c,31] where bond cleavage is seen. However, the proton signals undergo significant chemical shifts, suggesting a real change in the displacement of the metal center(s) effected by pyridine. The differences in the proton chemical shifts are more pronounced for the (TPP)Rh unit. All protons are downfield deshielded, with *pyrrolic*, *o′-endo*, and *m′-endo* protons (which are very close to the center of the magnetic anisotropy) experiencing the largest deshielding. This fact suggests that those protons experience a different chemical environment caused by the coordination of pyridine to rhodium and a change in its position with respect to the porphinato core. Again, evaporation of pyridine-d_5 and dissolution of the solid in $CDCl_3$ gives the initial ^{1}H NMR spectrum of the dimer.

The photochemical properties of the (Porph)Rh−Tl(Porph′) complexes are extremely complicated in comparison to those of the similar (Porph)Rh−In(Porph′) derivatives,[6b] and several points concerning their behavior are still under investigation.

Summary

The family of complexes containing a single metal−metal bond has been expanded by the species described herein. As synthetic limitations are overcome, the entire range of metalloporphyrins will undoubtedly exhibit similar chemistry.

Acknowledgment. This research was supported by the Greek General Secretariat of Research and Technology through Grant No. 95 A/A 1946 and by NIH Grant GM-38401 (W.R.S.). We are grateful to Mr. D. Schifferl of the NMR Facility at the University of Notre Dame for his assistance in recording spectra on the 500-MHz NMR spectrometer.

IC971393E

(31) Wayland, B. B.; Balkus, K. J.; Farmos, M. D. *Organometallics* **1989**, *8*, 950.